

Analysis of RSS-based Location Estimation Techniques in Fading Environments

Andreas Fink, Helmut Beikirch

Rostock University, Department of Computer Science and Electrical Engineering, Rostock, Germany.
Email: {andreas.fink;helmut.beikirch}@uni-rostock.de

Abstract—Distance estimation techniques based on RSS (received signal strength) measurements put low demand on the hardware and software complexity of the infrastructure components. Based on several distance calculations a location estimation algorithm is used to compute the position of an unknown node. The algorithms differ in their complexity, expressed by the need of computation time, and in the achievable accuracy of the position estimation. Experimental results in a real life indoor scenario with 2.4 GHz RF transceivers and multipath fading channels show that an approximative location estimation algorithm like an extended centroid localization method can reach a higher accuracy than an exact mathematic least squares approach, even though the resource-aware centroid localization method has a significant lower complexity than the least squares approach.

Index Terms—Indoor Localization, Signal Fading, 2.4 GHz ISM Radio, Received Signal Strength Readings, Centroid Location Estimation, Linear Least Squared Error Estimator.

I. INTRODUCTION

Indoor local positioning systems are ubiquitous and can be found in nearly every area of modern life. They can be used for the navigation of pedestrians in indoor areas or urban canyons where the availability of the global positioning system (GPS) is limited [1]. Another possible application is described in [2] where we have proposed a local positioning system based on received signal strength (RSS) measurements of radio frequency (RF) signals for the monitoring of maintenance staff in the underground longwall coal mining.

A basic classification of localization techniques is given in Fig. 1. The systems can be divided according to their physical measurement domain. The use of directional sensors like infra-red (IR), ultrasound, optical and magnetic systems is limited to line-of sight (LOS) scenarios. Typical indoor environments are often obstructed with many non-line-of sight (NLOS) conditions and thus make it challenging to get a reliable position information. An inertial navigation system (INS) or an RF localization system can be used for heavy obstructed NLOS scenarios [3], while the RF ranging sensors are known to be more error-prone due to the multipath fading effects [4],[5]. Nevertheless, RSS-based distance estimation techniques put low demand on the hardware and software complexity of the infrastructure components and thus, are widely distributed. E.g. the WLAN-based Horus system [6], RADAR system [7] or the commercial Ekahau location engine use RSS measurements.

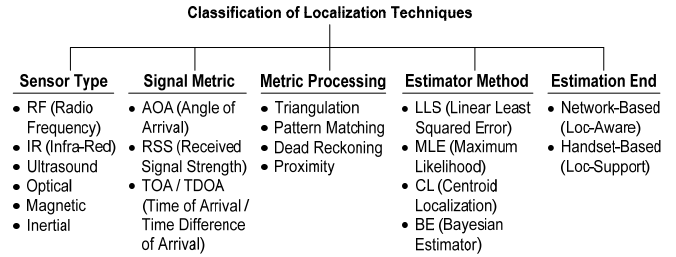


Fig. 1. Taxonomy of localization techniques according to the used sensor, the signal processing and the location estimator. Source: Own elaboration

Beside RSS measurements also time of flight measurements (TOA, TDOA) or direction of arrival measurements (AOA) are used as an RF signal metric to calculate the distance between the transmitter and the receiver. The disadvantage is the need of additional hardware and software components. E.g. precise timers are required for the synchronization of TOA and TDOA techniques [8]. For a more robust location information also hybrid positioning systems with a multisensor data fusion are commonly used [9],[10]. The fusion of a radio-based system with an INS is known to be more robust than each single system and can provide a more precise localization with a moderate hardware and software effort [11].

Another classification of localization systems is given by the estimation end. On one side there are handset-based techniques where the mobile unknown node (blind node, BN) computes the position. On the other side network-based techniques are used for energy aware systems where the energy-consuming computations are realized on one of the reference nodes (RNs). There exist many different algorithms to compute the position of an unknown node using a set of distance estimations. According to the achievable accuracy of the position estimation the algorithms are divided into exact methods (e.g. triangulation with least squared error estimator or maximum likelihood estimator) and approximative methods (e.g. proximity with centroid localization, dead reckoning with a Bayesian estimator).

A good overview with a comparison of the accuracy and the coverage of the different indoor positioning techniques is given in [12]. A more general taxonomy of localization systems can be found in [13].

In [14] we investigated the influence of a diversity platform and a plausibility filter on the accuracy of an RSS-based localization system. The sensor fusion of the RSS-based

system and an INS was presented in [2]. Our present work focuses on fault-tolerant location estimation algorithms for RSS-based systems which enable an adequate accuracy at minimum costs. The main issue is to find an algorithm which can provide a position information for the error-prone RSS input values. At the same time the main advantage of the RSS-based localization technique – the low complexity of the infrastructure components – have to be fulfilled by the location estimation algorithm.

In section II, the propagation of RF signals in indoor scenarios is explained and a path loss model is derived. The results from a path loss measurement in a real life scenario are presented and compared to the theoretical model. In section III, different location estimation techniques are discussed with a focus on range-based centroid localization methods. In section IV, the performance of the different location estimation techniques is evaluated by experimental results of a dynamic tracking measurement on a motion test track. In the last section V, the results are discussed and investigated in terms of an outlook for further system developments.

II. INDOOR RF SIGNAL PROPAGATION

A. Path Loss Model

Without any disturbances (free space propagation) the distance-depending path loss shows a logarithmic dropping of power with a linear increasing distance according to the Log-distance path loss model. With (1) the average path loss $\overline{PL}(d)$ (in dBm) over a distance d is given by the reference path loss $PL(d_0)$ over a reference distance d_0 and the environment-specific propagation coefficient n .

$$\overline{PL}(d) = PL(d_0) + 10n \log\left(\frac{d}{d_0}\right). \quad (1)$$

The value of $PL(d_0)$ is influenced by the effective radiated power (ERP) of the RF transmitter and the gain of the transmitting and receiving antenna. For an IEEE 802.15.4 compliant 2.4 GHz ISM transceiver with an output power of +10 dBm we have investigated a $PL(d_0)$ of -67 dBm at $d_0 = 1$ m.

The value of n is influenced by the specific environmental propagation conditions and the used frequency. In [15] and [16] values for n between 1.8 and 3.2 are given for obstructed indoor environments and frequencies between 900 MHz and 4.0 GHz. In Fig. 2 the average path loss $\overline{PL}(d)$ for these two values of n are shown on the left as a function of the distance between transmitter (TX) and receiver (RX).

In obstructed indoor environments not only NLOS conditions but multipath signal fading affect the RF signal propagation. Multipath fading becomes apparent by a significant short-term variation of the RSS values in the case the TX or RX antenna are moved in the order of the wavelength (e.g. a few centimeters). The fading follows a Rayleigh distribution. The PDF of the distribution is defined as follows:

$$f(x, \theta) = \begin{cases} \frac{x e^{-\frac{x^2}{2\theta^2}}}{\theta^2} & , x \geq 0 \\ 0 & , x < 0 \end{cases}, \quad (2)$$

where the maximum likelihood estimator of θ is defined as

$$\hat{\theta} \approx \sqrt{\frac{1}{2N} \sum_{i=0}^N x_i^2}. \quad (3)$$

The expectation value $E(X_r)$ of the Rayleigh distribution is defined as

$$E(X_r) = \theta \sqrt{\frac{\pi}{2}}. \quad (4)$$

The PDFs in Fig. 2 on the right show the path loss distribution $PL(d_{RX})$ at the RX antenna for a fixed distance d_{RX} between RX and TX antenna. The two distributions represent the corresponding RSS variations for the two different path loss coefficients $n = 1.8$ and $n = 3.2$. For $n = 1.8$ the expectation value and the maximum likelihood estimator of the Rayleigh distribution are close together. For increasing n the probability for RSS values below the expectation value increases. Furthermore, the Rayleigh distributed fading in NLOS indoor environments is characterized by frequent signal dropouts. The dropouts are assumed to be randomly distributed and can be as large as 40 dBm [16].

The distance dependent path loss from (1) is an average value and therefore not suitable to describe a real channel. For obstructed indoor environments a zero-mean Gaussian random variable X_σ with standard deviation σ is added to the average path loss:

$$PL(d) = PL(d_0) + 10n \log\left(\frac{d}{d_0}\right) + X_\sigma. \quad (5)$$

X_σ can be described with the standard deviation σ of the Rayleigh distribution which is defined as follows:

$$\sigma = \sqrt{\frac{4 - \pi}{2}} \theta. \quad (6)$$

With (1) and a reference path loss $PL(d_0)$ at a distance $d_0 = 1$ m the distance between transmitter and receiver can be calculated with

$$d = 10^{\left(\frac{PL(d_{RX}) - PL(d_0)}{10n}\right)}, \quad (7)$$

where $PL(d_{RX})$ is the path loss measured at the receiver.

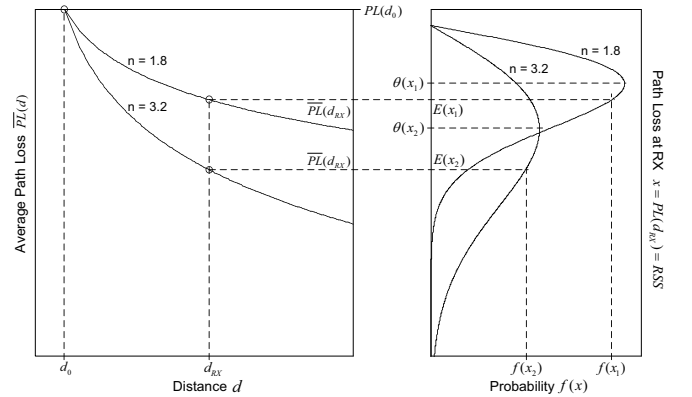


Fig. 2. Log-normal path loss model (left) and PDFs (right) for two different fading channel estimations ($n = 1.8$ and $n = 3.2$). Source: Own elaboration

B. Real Life Path Loss Measurement

To investigate the path loss in fading environments we have carried out an indoor measurement on a motion test track in an industrial like test hall (cf. Fig. 3). The linear track of the TX node starts at the end position B, ends at the end position A and has an overall length of 9.6 m. The RX node is fixed at a distance of 1.4 m to the end position B while the TX node can move along the track with a maximum speed of 5 m/s. For our path loss measurement the TX speed is set to 0.27 m/s and the TX transmission rate is 5 Hz. For the given dynamic behavior of the TX node the distance between RX and TX node changes approximately 0.05 m between two transmissions. Since this value is smaller than the 2.4 GHz wavelength of approximately 0.12 m we expect to figure out the multipath fading behavior with this configuration. For an explicit multipath propagation we installed metallic reflecting walls next to the track.

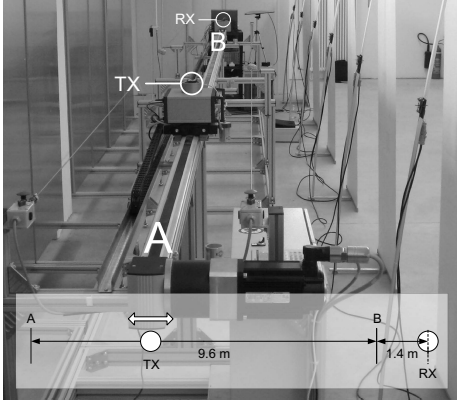


Fig. 3. Path loss measurement setup on a motion test track in an obstructed test hall. Source: Own elaboration

The RSS over a distance of 11 m is shown in Fig. 4 where the small-scale fading due to the multipath propagation is pointed out. As mentioned above, the reference path loss $PL(d_0)$ at a distance of $d_0 = 1$ m between TX and RX antenna is -67 dBm for the used IEEE 802.15.4 compliant 2.4 GHz RF transceiver. The resulting path loss coefficient $n = 2.62$ is a typical value for fading environments. The destructive interferences of different multipath signals lead to abrupt signal dropouts where the signal sometimes even falls below the receiver's sensitivity level S_{min} and the transmitted information gets lost. Even if the information arrive the receiver, the measured RSS is strongly fluctuating. The variation of the RSS values for the given path loss measurement is shown in the histogram in Fig. 5.

The RSS variation follows a Rayleigh distribution with $E(X_r) = 0$ dBm and $\sigma = 5.70$ dBm. The RSS variation for all measured values is 30 dBm. With (7) a path loss of 30 dBm corresponds to a spatial shift between 1 m and more than 25 m. Thus, for a localization a measured RSS can not be assigned to a single distance. The error-prone behavior of RSS-based distance estimations should be taken into account at the algorithmic level of the location estimation.

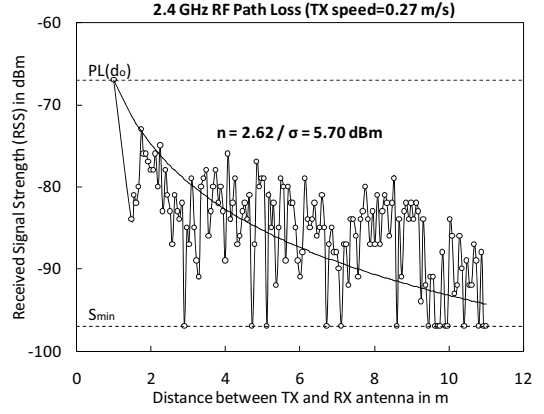


Fig. 4. Path loss for 2.4 GHz over a distance of 11 m (150 RSS samples, TX speed = 0.27 m/s, 5 Hz update rate). Source: Own calculation

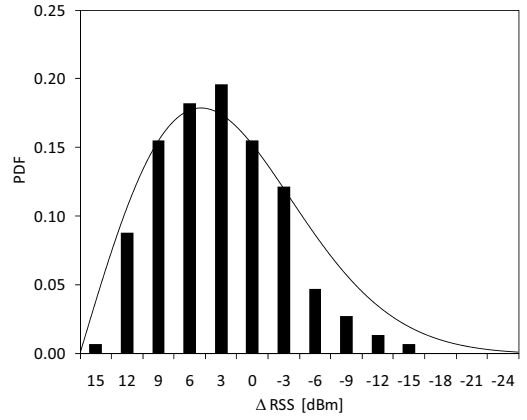


Fig. 5. RSS distribution for 2.4 GHz path loss measurement and corresponding Rayleigh distribution. Source: Own calculation

III. LOCATION ESTIMATION TECHNIQUES

A classification of localization techniques according to the metric processing and the estimation method is given in Fig. 1. For a dynamic environment with moving obstacles the scene analysis (pattern matching) technique is challenging because it is based on a static a priori knowledge of the environment. A metric processing with triangulation of a set of distance estimations or a proximity method are more useful for an obstructed indoor environment with randomly changing propagation conditions. In the following two specific location estimation algorithms for range-based systems are presented and compared.

A. Linear Least Squared Error

The method of linear least squared (LLS) errors is a mathematically exact approach for the triangulation technique using a measurement set of distances or angles between a mobile BN and a number of fixed RNs. For a two-dimensional localization the distance to three RNs is required to compute the position of the BN. With more than three RNs the resulting linear system is overdetermined. In Fig. 6 a configuration of four RNs is shown. The circles, representing the estimated

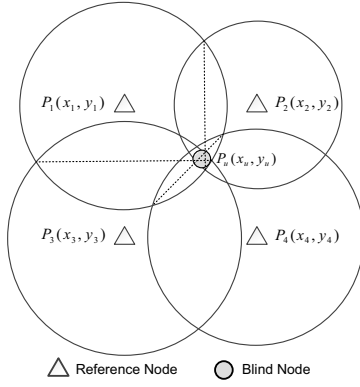


Fig. 6. Linear least squared error method for a two-dimensional localization using a set of four reference nodes (RN1 is used for the linearization). Source: Own elaboration

distances, are not crossing each other in one single point. Thus, there exist no exact solution for the system.

The LLS approach minimizes the sum of squared errors of the erroneous distance estimations $\tilde{d}_j (j = 2, \dots, m_{RN})$ to m RNs to solve the following system of equations:

$$(x_u - x_j)^2 + (y_u - y_j)^2 = \tilde{d}_j^2. \quad (8)$$

For the solution first a linearization of (8) is performed by subtracting the location of the first RN from all other equations [17]. The new systems of equations has the matrix form $\mathbf{Ax} = \mathbf{b}$ with

$$\mathbf{A} = \begin{pmatrix} 2x_1 - 2x_2 & 2y_1 - 2y_2 \\ 2x_1 - 2x_3 & 2y_1 - 2y_3 \\ \dots & \dots \\ 2x_1 - 2x_n & 2y_1 - 2y_n \end{pmatrix}, \quad (9)$$

$$\mathbf{b} = \begin{pmatrix} \tilde{d}_2^2 - \tilde{d}_1^2 + x_1^2 - x_2^2 + y_1^2 - y_2^2 \\ \tilde{d}_3^2 - \tilde{d}_1^2 + x_1^2 - x_3^2 + y_1^2 - y_3^2 \\ \dots \\ \tilde{d}_n^2 - \tilde{d}_1^2 + x_1^2 - x_n^2 + y_1^2 - y_n^2 \end{pmatrix}, \quad (10)$$

$$\mathbf{x} = \begin{pmatrix} x_u \\ y_u \end{pmatrix}. \quad (11)$$

The estimated position of the BN can be calculated with the LLS method, solving the following equation:

$$\begin{pmatrix} \hat{x}_u \\ \hat{y}_u \end{pmatrix} = (\mathbf{A}^T \mathbf{A})^{-1} (\mathbf{A}^T \mathbf{b}). \quad (12)$$

B. Centroid Localization

Centroid localization (CL) is a proximity based technique to determine the position of a BN with the help of certain RNs with minimum software efforts. The basic CL algorithm as a simple range-free implementation uses the link to several RNs as sensor input for a rough location estimation [18]. In Fig. 7 a scenario with four RNs is shown. Under the assumption of entire uniform circular communication ranges, the BN is

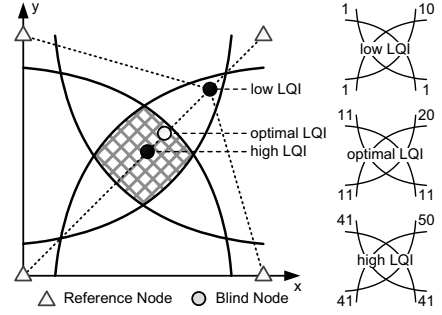


Fig. 7. Centroid localization approach showing the influence of the LQI distribution on the position estimation. Source: [19]

located inside the shaded area when it has a link to all four RNs.

The general weighted centroid localization (WCL) approach uses a link quality indicator (LQI) to get a more precise location information [20]. For a range-based option of the WCL the RSS indicator (RSSI) values from various RNs can be used. The RSS values from all RNs are transformed into distances according to the Log-distance model and (7). The distance between RN number j and the BN at time instance i can be written as d_{ij} . The distances d_{ij} are transformed into weights w_{ij} according to (13).

$$w_{ij} = \frac{1}{(d_{ij})^g} \quad (13)$$

Similar to the path loss coefficient n , the weighting factor g depends on the environmental conditions. From previous measurements in obstructed indoor environments the weighting factor was determined between 2.2 and 3.8.

The BN's position is given by the weighted positions of the RNs. The accuracy depends on the subfield of the regarding area (center or border) and the relationship between relative and absolute LQI values. For low LQIs the BN might be located near a dominating RN. For high LQIs the advantage of the weighting gets lost and the WCL reaches similar results to CL.

In [14] we have proposed the selective adaptive weighted centroid localization (SAWCL) approach, which enables a further improvement of the accuracy by an adaption of the weights according to their statistical distribution. Looking at Fig. 7, for low LQIs all of the weights are raised by a specific fraction, for high LQIs they are reduced to increase the relative difference of the weights. The BN's two-dimensional position $P_i(x, y)$ at the time instant i is computed with the modified weights w'_{ij} and the fixed positions $B_j(x, y)$ of the RNs according to

$$P_i(x, y) = \frac{\sum_{j=1}^m (w'_{ij} \cdot B_j(x, y))}{\sum_{j=1}^m w'_{ij}}. \quad (14)$$

IV. EXPERIMENTAL RESULTS

A one-dimensional tracking measurement is used to compare the LLS estimator and the SAWCL algorithm in terms

of accuracy and complexity. A typical application for the one-dimensional localization case is the monitoring of maintenance staff in the underground longwall coal mining environment where automatically moving electro-hydraulic shields need to be stopped when a miner is located in front of them. The importance of the availability of the localization and tracking for a secure and productive mining strategy was investigated in [2]. The issues for the actual measurements are the accuracy and the effort of different location estimation algorithms.

The measurement setup is based on previous tracking measurements in an overground longwall mining test bed with eight electro-hydraulic shields and a conveyor belt in front of them [2]. For the actual tracking measurement we use the motion test track described at the path loss measurement in section II-B. The main advantage of the motion test track towards the overground longwall test bed is the defined and flexible motion profile. The seven RNs are located 1.0 m next to the track with a distance of 2.0 m between the nodes. The BN performs periodic movements on the motion test track according to the motion profile shown in Fig. 8. The duration of one movement from position A to B and back to A is 65 s.

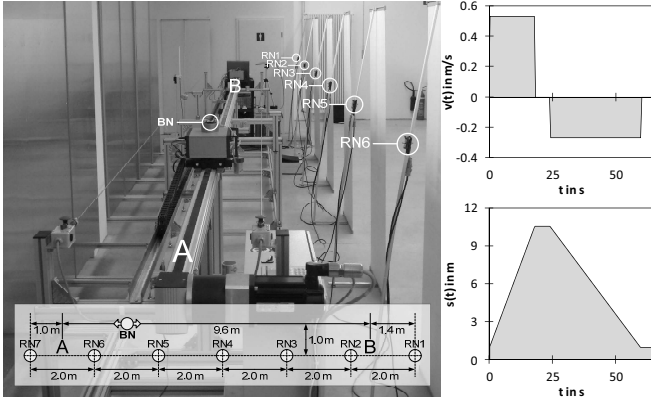


Fig. 8. Measurement setup on a motion test track in an obstructed test hall (velocity and position profiles show one A-B-A motion cycle, $T = 65$ s). Source: Own elaboration

In Fig. 9 the 99th percentile of the SAWCL's location estimation error (LEE) for different values of the weighting factor g is shown. The LEE shows two local minima around $g = 3.0$. The absolute minimum LEE is reached for $g = 3.8$.

To have a look at the LEE of the SAWCL and the LLS we compare the CDF of both algorithms in Fig. 10 where the weighting factor for the SAWCL algorithm was set to $g = 3.8$. The corresponding values for the maximum, median and 95th percentile of the LEE are given in Table I. The median error of both estimators is below 0.72 m. For a reliable tracking application it is necessary to have a look at the maximum error or at least the 95th percentile. The $LEE_{95\%}$ of the LLS estimator is three to four times higher than for the approximative SAWCL. At the same time the runtime complexity for the SAWCL calculations is nearly five times lower than for the LLS method.

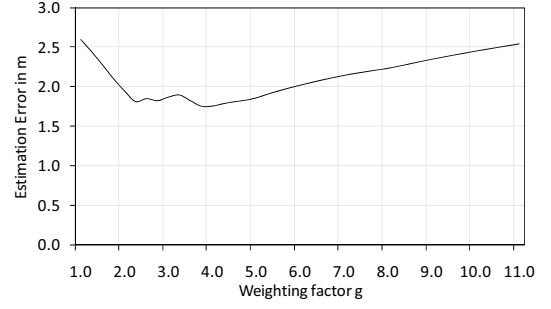


Fig. 9. 99th percentile of the location estimation error (LEE) for the SAWCL algorithm as a function of the weighting factor g . Source: Own elaboration

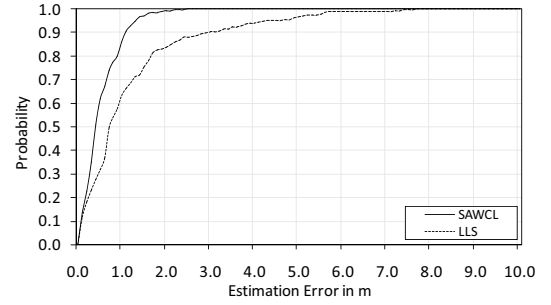


Fig. 10. Cumulative distribution functions for the location estimation error of a 9.6 m tracking measurement using the LLS estimator compared to the SAWCL algorithm ($g = 3.8$). Source: Own calculation

V. CONCLUSION AND FUTURE WORK

The results from a real life path loss measurement show the error-prone behavior of the RSS values in obstructed indoor environments. The fading characteristics require a fault tolerant location estimation technique for an RSS-based indoor localization. The experimental results on the motion test track show the performance of the approximative SAWCL compared to the LLS approach. The significant advantage of the SAWCL benefits from the centroid approach. Hence, the unknown BN is always located on the line between the first and the last RN. With the LLS approach the BN position is often estimated outside the track, despite of the higher complexity of the LLS calculations. The evaluation of the weighting factor g for the SAWCL algorithm shows that there exists an optimum value where the LEE has a minimal value for 99% of the measurement value range. Like the path loss coefficient n the weighting factor g depends on the environmental conditions.

TABLE I
PERFORMANCE COMPARISON OF DIFFERENT ESTIMATION TECHNIQUES
(LEE - LOCATION ESTIMATION ERROR IN METERS, PERCENTAL RUNTIME
COMPLEXITY RELATIVE TO THE SAWCL)

	LLS	SAWCL
LEE_{med}	0.72 m	0.33 m
σ_{LEE}	1.37 m	0.43 m
$LEE_{95\%}$	4.25 m	1.29 m
LEE_{max}	6.24 m	1.85 m
Complexity	480 %	100 %

The measurements show the importance of an adapted estimation strategy for error-prone distance estimations from fading channel RSS readings. Beside RSS measurements, also other range-based techniques using TOA or TDOA measurements could reach good results with the fault-tolerant centroid localization approach.

Our further research focuses on the investigation of additional estimation techniques, e.g. the maximum likelihood estimator (MLE) or a Bayesian estimator using a Kalman filter. The experimental results of these techniques will extend the given comparison, whereas a more sophisticated comparison of the complexity – including runtime, memory space and communication overhead – will be used.

REFERENCES

- [1] Yutaka Inoue, Akio Sashima, and Koichi Kurumatani. Indoor positioning system using beacon devices for practical pedestrian navigation on mobile phone. In *Ubiquitous Intelligence and Computing*, volume 5585 of *Lecture Notes in Computer Science*, pages 251–265. Springer Berlin / Heidelberg, 2009.
- [2] A. Fink, H. Beikirch, M. Voss, and C. Schroeder. RSSI-based indoor positioning using diversity and inertial navigation. In *IEEE International Conference on Indoor Positioning and Indoor Navigation (IPIN)*, pages 1–7, 2010.
- [3] H. Wang, H. Lenz, A. Szabo, J. Bamberger, and U.D. Hanebeck. WLAN-based pedestrian tracking using particle filters and low-cost MEMS sensors. In *4th IEEE Workshop on Positioning, Navigation and Communication (WPNC)*, pages 1–7. IEEE, 2007.
- [4] E. Elnahrawy, Xiaoyan Li, and R.P. Martin. The limits of localization using signal strength: A comparative study. In *IEEE Sensor and Ad Hoc Communications and Networks (SECON)*, pages 406 – 414, 2004.
- [5] Kamin Whitehouse, Chris Karlof, and David Culler. A practical evaluation of radio signal strength for ranging-based localization. *SIGMOBILE Mobile Computing and Communications Review*, 11:41–52, January 2007.
- [6] M. Rehim. *Horus: A WLAN-based Indoor Location Determination System*. PhD thesis, University of Maryland, 2004.
- [7] Paramvir Bahl and Venkata N. Padmanabhan. RADAR: an in-building RF-based user location and tracking system. pages 775–784, 2000.
- [8] W.-S. Jang and M. J. Skibniewski. A wireless network system for automated tracking of construction materials on project sites. *Journal of Civil Engineering and Management*, 2008.
- [9] C. Hide, T. Botterill, and M. Andreotti. Low cost vision-aided IMU for pedestrian navigation. In *Ubiquitous Positioning Indoor Navigation and Location Based Service (UPINLBS)*, 2010, pages 1 –7, 2010.
- [10] L. Johannes, J. Degener, and W. Niemeier. Set-up of a combined indoor and outdoor positioning solution and experimental results. In *Indoor Positioning and Indoor Navigation (IPIN), 2010 International Conference on*, pages 1 –6, 2010.
- [11] Francois Caron, Emmanuel Duflos, Denis Pomorski, and Philippe Van-heeghe. GPS/IMU data fusion using multisensor Kalman filtering: introduction of contextual aspects. *Inf. Fusion*, 7:221–230, June 2006.
- [12] T. Kohoutek, R. Mautz, and A. Donaubaue. Real-time indoor positioning using range imaging sensors. In *Proceedings of SPIE Photonics*, volume 7724, 2010.
- [13] J. Hightower and G. Boriello. *A survey and taxonomy of location systems for ubiquitous computing*. Technical report, University of Washington, Department of Computer Science and Engineering, 2001.
- [14] A. Fink, H. Beikirch, and M. Voss. Improved indoor localization with diversity and filtering based on received signal strength measurements. *International Journal of Computing*, Vol. 9(Issue 1):pages 9–15, 2010.
- [15] T.S. Rappaport and C.D. McGillem. Uhf fading in factories. *IEEE Journal on Selected Areas in Communications*, 7(1):40 –48, January 1989.
- [16] T.S. Rappaport. *Wireless Communications – Principles and Practice*. Prentice Hall PTR, 2002.
- [17] William Navidi, William S. Murphy, Jr., and Willy Hereman. Statistical methods in surveying by trilateration. *Comput. Stat. Data Anal.*, 27:209–227, April 1998.
- [18] Nirupama Bulusu John, John Heidemann, and Deborah Estrin. GPS-less low cost outdoor localization for very small devices. *IEEE Personal Communications Magazine*, 7:28–34, 2000.
- [19] R. Behnke and D. Timmermann. AWCL: Adaptive weighted centroid localization as an efficient improvement of coarse grained localization. In *5th Workshop on Positioning Navigation and Communication*, pages 243–250, 2008.
- [20] Jan Blumenthal, Frank Reichenbach, and Dirk Timmermann. Position estimation in ad-hoc wireless sensor networks with low complexity. In *2nd Workshop on Positioning, Navigation and Communication (WPNC)*, pages 41–49, 2005.